Nuclear Instruments and Methods in Physics Research A 787 (2015) 236–239

Contents lists available at ScienceDirect

Nuclear Instruments and Methods in Physics Research A

journal homepage: www.elsevier.com/locate/nima

Fabrication, characterization and testing of silicon photomultipliers for the *Muon Portal* Project

P. La Rocca [a,b,*], S. Billotta [c], A.A. Blancato [a], D. Bonanno [a], G. Bonanno [c], G. Fallica [d], S. Garozzo [c], D. Lo Presti [a,b], D. Marano [c], C. Pugliatti [a,b], F. Riggi [a,b], G. Romeo [c], G. Santagati [a,b], G. Valvo [d]

[a] *Dipartimento di Fisica e Astronomia - Catania, Italy*
[b] *INFN - Sezione di Catania, Italy*
[c] *INAF - Osservatorio Astrofisico di Catania, Italy*
[d] *STMicroelectronics - Catania, Italy*

ARTICLE INFO

Available online 16 December 2014

Keywords:
Silicon photomultiplier
Scintillator
Tracking detector

ABSTRACT

The *Muon Portal* is a recently started Project aiming at the construction of a large area tracking detector that exploits the muon tomography technique to inspect the contents of traveling cargo containers. The detection planes will be made of plastic scintillator strips with embedded wavelength-shifting fibres. Special designed silicon photomultipliers will read the scintillation light transported by the fibres along the strips and a dedicated electronics will combine signals from different strips to reduce the overall number of channels, without loss of information. Different silicon photomultiplier prototypes, both with the *p-on-n* and *n-on-p* technologies, have been produced by STMicroelectronics during the last years. In this paper we present the main characteristics of the silicon photomultipliers designed for the *Muon Portal* Project and describe the setup and the procedure implemented for the characterization of these devices, giving some statistical results obtained from the test of a first batch of silicon photomultipliers.

1. Introduction

In the last years, the demand for increasing the control security at borders and ports has lead to the development of innovative and reliable techniques to inspect the contents of traveling containers. One of the most promising technique is the so-called muon tomography: by measuring the deflection suffered by cosmic muons when traversing high-*Z* materials, it is possible to reconstruct a 3D image of the volume to be inspected and detect the presence of fissile (U, Pu) samples in a reasonable amount of time (a few minutes), compatible with the requirement of a fast inspection technique [1–4].

The *Muon Portal* Project plans to build a prototype for the inspection of real size 20 in.-Box containers by using the muon tomography technique [5]. The detection setup is based on eight position-sensitive planes (giving *X*- and *Y*-coordinates), four placed below and four above the volume to be inspected (see Fig. 1), with good tracking capabilities for the charged particles (muons and electrons).

The detection planes are segmented into strips of extruded plastic scintillators with wavelength-shifting (WLS) fibres (Kuraray Y11(200)M [6]) to transport the light produced in the extruded scintillator material (produced by AMCRYS-H company [7]) to the photo-sensors at one of the fibre ends, in order to optimize the amount of collected photons, still maintaining at a reasonable level the cost and the size of the detection setup [8–11].

The photo-sensors used are silicon photomultipliers custom-made by STMicroelectronics in order to fit the size of the WLS fibres and match their emission spectrum.

In this paper we describe the test and the characterization of the silicon photomultipliers produced for the *Muon Portal*. The final chip design is reported in Section 2, while the results of the optical and electrical characterization are described in Section 3. Finally, the quality assurance procedure and the selection phase are discussed in Section 4.

2. Silicon photomultiplier technology

The silicon photomultiplier (SiPM) prototype designed for the *Muon Portal* Project has to maximize the photon detection efficiency and the cell fill factor, as well as to ensure a low cross-talk and dark count rate. Different SiPM prototypes (1 mm^2 area), both with the *p-on-n* and *n-on-p* technologies, have been produced by

* Corresponding author at: Dipartimento di Fisica e Astronomia - Catania, Italy.
E-mail address: paola.larocca@ct.infn.it (P. La Rocca).

http://dx.doi.org/10.1016/j.nima.2014.12.026
0168-9002/

STMicroelectronics before the mass production. The prototypes have been fully characterized (both from an electrical and optical point of view) at different temperatures and working conditions in order to choose the best device.

The layout of the final chip is based on *n-on-p* technology and embeds 4 independent round shaped SiPMs, as shown in Fig. 2.

Actually the chip contains two types of SiPMs, which differ for their cell pitch: the MUON60 type has 548 cells with 60 μm pitch, whereas the MUON75 type has 320 cells with 75 μm pitch. The SiPMs have one pad for the cells biasing, one pad for the common substrate electrode and one pad for the breakdown check (connected to an independent diode without quenching resistor). The main characteristics of the MUON60 and MUON75 SiPMs are listed in Table 1.

Custom supports placed at one end of the strips allow us to route and align the WLS fibres that are then polished and finally coupled to the SiPM chip. Since each strip is read out by two different WLS fibres, the total number of SiPMs needed for the whole detector is 9600.

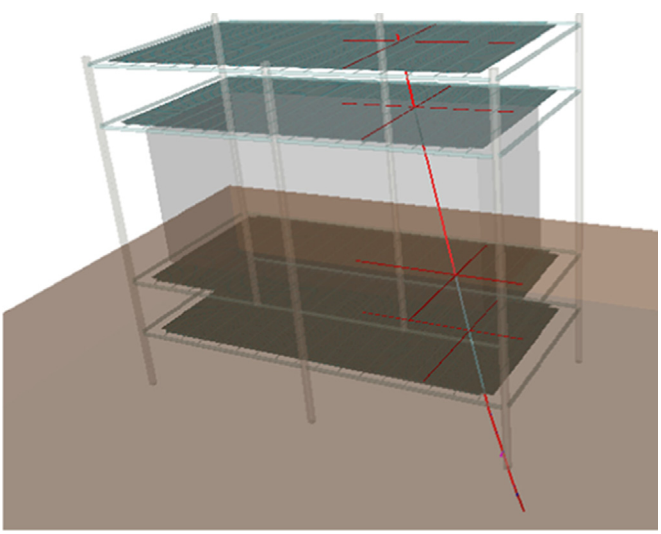

Fig. 1. View of the *Muon Portal* detector illustrating the detection of a cosmic muon passing through the detector.

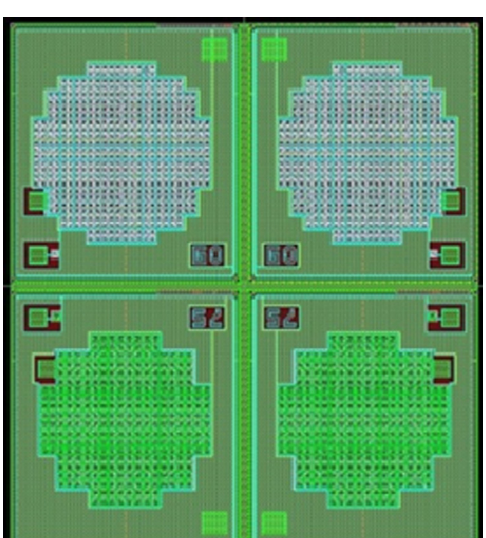

Fig. 2. Layout of the single module (upper row: MUON60; lower row: MUON75).

Table 1
Features of the MUON60 and MUON75 devices. The last 5 parameters are evaluated at the optimal operation overvoltage OV.

Parameter	MUON60	MUON75
Sensitive area size (mm^2)	1.97	1.80
Number of cells	548	320
Cell capacitance (fF)	280	445
Cell quenching resistor (kΩ)	550	800
Cell fill factor (%)	67.4	73.8
Typical breakdown voltage (V)	27.4	27.4
Optimal operation OV (V)	3–4	3–4
Gain	6.8×10^6	7.6×10^6
Typical dark current (μA)	~ 2	~ 2
Typical dark count rate (MHz)	~ 2	~ 2
Optical crosstalk (%)	1.5	1.5
Photon detection efficiency at $\Delta\lambda = 500$–550 nm (%)	28	31

3. Optical and electrical characterization

A preliminary R&D activity has been carried out before starting the mass production of the photo-sensors. Many prototypes have been produced and characterized in terms of optical and electrical characterization [10]. As an example, Fig. 3 shows the Photon Detection Efficiency (PDE) of the prototype SMP10H5-60N that uses the same technology of the final MUON60 but with a reduced area (1 mm^2). The experimental setup used to perform the PDE measurement consists of a Xenon lamp as luminous source, a system to select the wavelength of interest and a beam splitter to direct the monochromatic radiation towards an integrating sphere hosting a calibrated reference photodiode and the SiPM under test. The sphere was used to obtain a uniform illumination on both detectors, while the reference photodiode, traced by the National Institute of Standard Technology (NIST), served to measure the flux of the incident radiation on the SiPM. For PDE measurements we used the photon counting method. Furthermore it should here be remarked that optical cross-talk effects are not accounted for in the adopted photon counting technique for determining the detector PDE, as a 0.5-pe threshold is applied to all triggered pulses, such that simultaneous pulses are always measured as a single pulse (for further details refer to references [12,13]). In the range $\Delta\lambda = 500$–550 nm (which corresponds to the main emission region of the Kuraray WLS fibre) this device showed the higher PDE (with respect to other prototypes) ranging from 30% to 40%.

Once the SiPM technology was chosen, the final chips with the 4 SiPMs embedded have been fabricated and some samples were fully characterized. The chips were put into a light-tight box and were illuminated with a blue light driven from a pulsed LED through an optical fibre. The SiPMs were biased and the output signal was amplified by the use of a CAEN SP5600 General Purpose Power Supply and Amplification Unit. A CAEN DT5720A fast digitizer (2 Channels, 250 MS/s, 12 bit) allowed us to display the signals, evaluate the output charge of the sensor under test and measure the Dark Count Rate (DCR) in the absence of light. All these data were processed to extract additional information, such as the gain and the resolution power of the system. As an example, the DCR as a function of the overvoltage is reported if Fig. 4, whereas Fig. 5 shows the gain of MUON60 as a function of the overvoltage.

4. SiPM classification

In the final design the SiPMs will be optically coupled to the polished fibres and will be enclosed inside a hermetic box, in order to be operated in dark conditions at a controlled temperature. Moreover, to improve the uniformity of the SiPMs response along

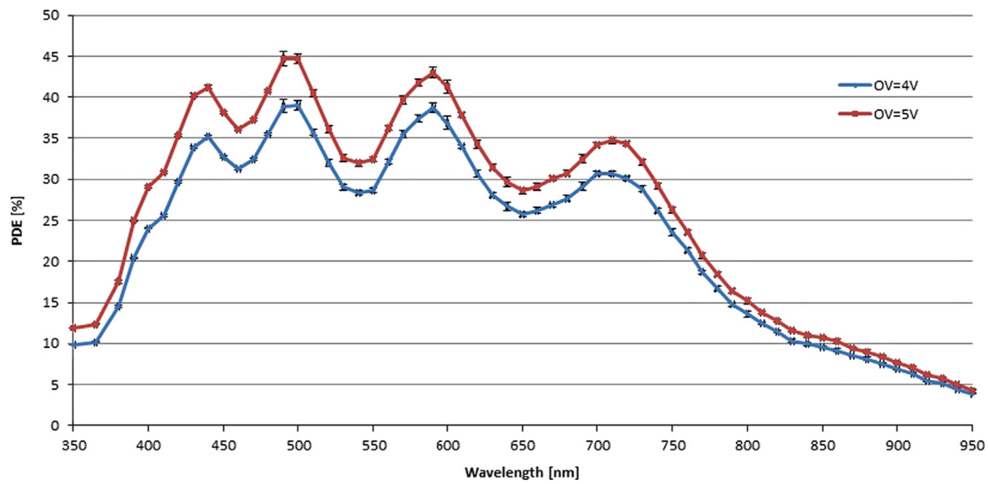

Fig. 3. PDE for SMP10H5-60N (temperature $T=28\ ^{\circ}$C).

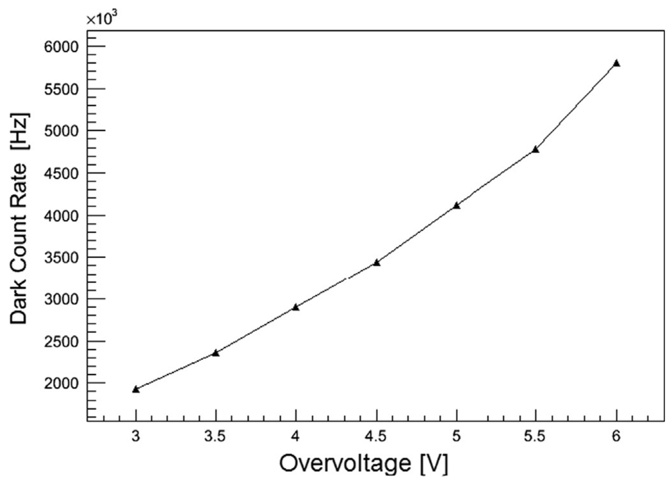

Fig. 4. Dark count rate of MUON60 SiPM as a function of overvoltage.

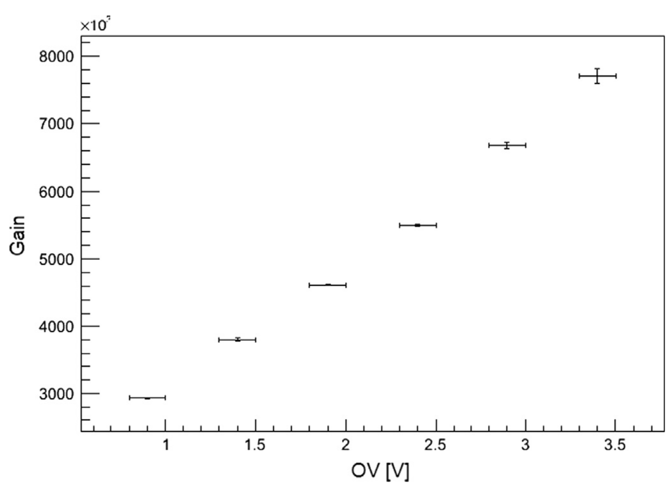

Fig. 5. Gain of MUON60 as a function of overvoltage.

the detection modules, the devices will be divided into groups, depending on their breakdown voltage. SiPMs with similar characteristics will be installed in the same region of the detector in order to set, for group of 10 SiPMs, the same bias voltage and threshold level. Finally, the thresholds will be remotely controlled and automatically varied to ensure the gain stability in case of temperature variation.

For this reason, the characterization of all the devices is necessary for their classification before the final assembling of the Portal. A batch of $\sim$10 000 SiPMs has been produced and encapsulated in a SMD optical package. A custom procedure has been implemented for the characterization of such devices. The setup is made of a black box where the device under test is placed inside a proper socket; the device is biased by a Keithley picoammeter/voltage source that is also used to read the current from the device and transmit data to a computer.

A LabVIEW program, running on a computer which communicates by RS-232 port with the Keithley device, has been developed for our purpose. A complete *I–V* curve is measured in an automatic way by setting the bias voltage and reading the corresponding current in the device. Starting from a bias voltage of 25 V up to 34 V in steps of 0.075 V, the program is able to find the Breakdown Voltage BV value for each SiPM under test by reading the corresponding current I_{BV}. As an example, in Fig. 6 the *I–V* curve is shown for 3 different devices: the first SiPM (on the left) fits all the quality requirements, the other 2 SiPMs are rejected due to quality cuts on the dark current.

After the construction of the *I–V* curve it is possible to reject those SiPMs not satisfying stringent criteria on the BV (i.e. a good compromise is $27\ V < BV < 29\ V$). Other testing criteria are applied to the current values corresponding to BV+5 V and BV−2 V and the goodness of a device is evaluated in a simple way, thanks to the switching of appropriate signaling LEDs on the acquisition panel. The data collected for a first batch of 2500 SiPMs have been analyzed. The selection criteria chosen have led to a rejection percentage of less than 20% that is compatible with what expected by previous tests on prototype devices. Fig. 7 shows the breakdown voltage distribution of the accepted devices, whereas Fig. 8 shows the dark current distribution (at OV=3 V and OV=4 V) of the same devices. The RMS value suggests a good uniformity within the batch tested.

5. Conclusions

The *Muon Portal* Project has just entered the construction phase and plans to arrive at the completion of the entire setup within mid-2015. The whole detector has been designed to inspect real-size containers and will cover an area of $\sim 18\ m^2$.

The fine segmentation of the detector requires the use of 9600 light output channels. For such a reason, the use of silicon photomultipliers as read-out photo-sensors was almost obligated,

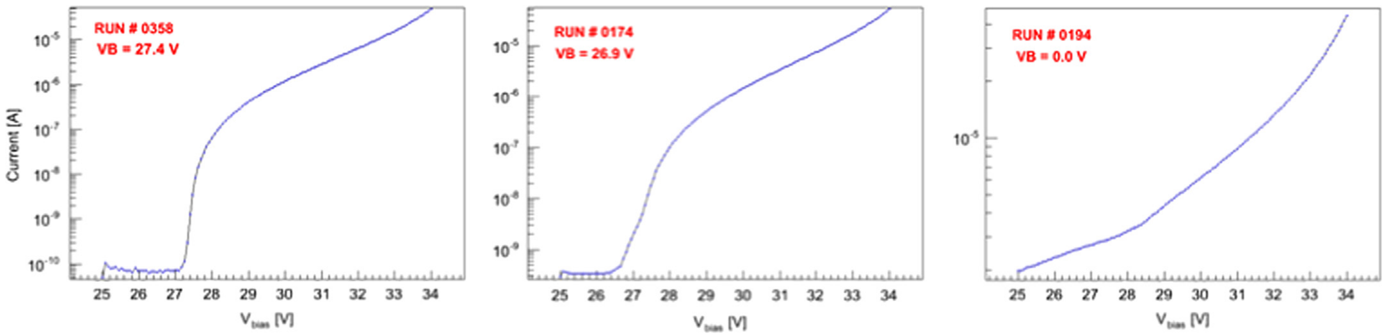

Fig. 6. *I–V* curve measured for 3 different devices: the first on the left corresponds to a SiPM accepted, the other 2 correspond to SiPMs that are rejected due to quality requirements on the dark current.

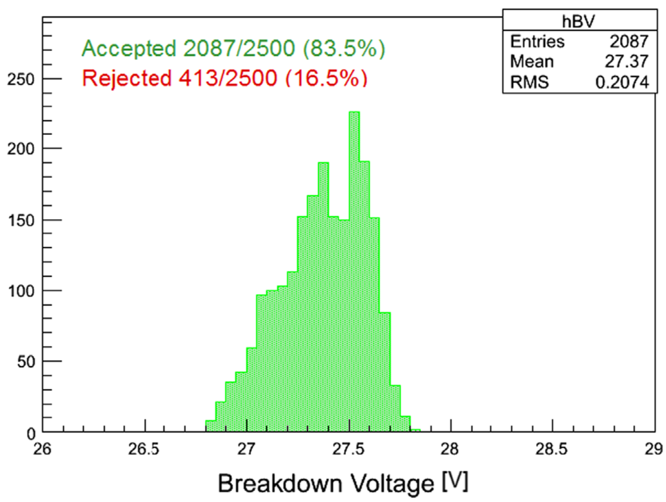

Fig. 7. Breakdown voltage distribution, measured over a sample of 2500 devices.

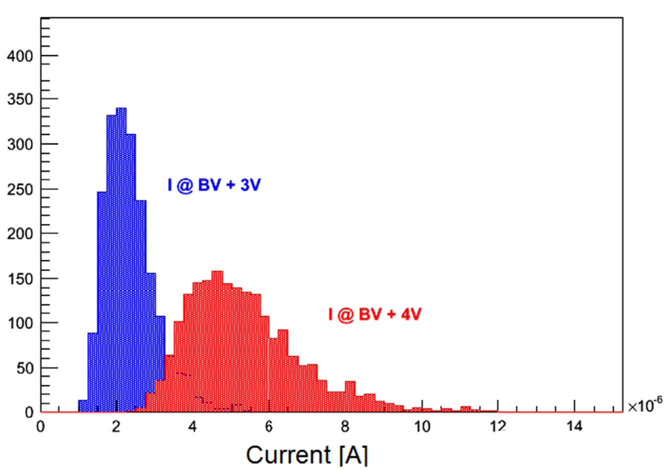

Fig. 8. Dark current distribution at OV=3 V(blue) and OV=4 V (red) of the accepted devices. (For interpretation of the references to color in this figure caption, the reader is referred to the web version of this paper.)

thanks to their compactness, cost-effectiveness and low voltage biasing.

It was chosen to use custom designed silicon photomultipliers in order to maximize the photon detection efficiency, the fill factor with a low cross-talk and dark count rate.

After a preliminary R&D phase, the whole batch of 10000 silicon photomultipliers has been produced. While a small sample was fully characterized to determine the optical and electrical properties, the measurement of the *I–V* characteristics is performed on each device in order to reject those silicon photomultipliers not satisfying the requirements imposed by the read-out electronics that will properly combine signals in groups of ten, thus reducing the number of output channels without loss of information [11].

References

[1] K.R. Borozdin, et al., Nature 422 (2003) 277. http://dx.doi.org/10.1038/422277a.
[2] W.C. Priedhorsky, et al., Review of Scientific Instruments 74 (2003) 4294. http://dx.doi.org/10.1063/1.1606536.
[3] K. Gnanvo, et al., Nuclear Instruments and Methods in Physics Research Section A 652 (2011) 16. http://dx.doi.org/10.1016/j.nima.2011.01.163.
[4] S. Pesente, et al., Nuclear Instruments and Methods in Physics Research Section A 604 (2009) 738. http://dx.doi.org/10.1016/j.nima.2009.03.017.
[5] ⟨http://muoni.oact.inaf.it⟩.
[6] ⟨http://kuraraypsf.jp/psf/ws.html⟩.
[7] AMCRYS-H, 60, Lenin ave, Kharkov, 310001, Ukraine.
[8] A. Antonuccio, et al., The Muon Portal Collaboration, IEEE Nuclear Science Symposium and Medical Imaging Conference Record (NSS/MIC) 6551049 (2012) 5–8. http://dx.doi.org/10.1109/NSSMIC.2012.6551049.
[9] S. Riggi, et al., The Muon Portal Collaboration, Journal of Physics—Conference Series 409 (2013) 012046. http://dx.doi.org/10.1088/1742-6596/409/1/012046.
[10] P. La Rocca, et al., The Muon Portal Collaboration, Journal of Instrumentation 9 (2014) C01056. http://dx.doi.org/10.1088/1748-0221/9/01/C01056.
[11] C. Pugliatti, et al., The Muon Portal Collaboration, Journal of Instrumentation 9 (2014) C05029. http://dx.doi.org/10.1088/1748-0221/9/05/C05029.
[12] G. Bonanno, et al., IEEE Sensors Journal 14 (2014) 3557. http://dx.doi.org/10.1109/JSEN.2014.2328621.
[13] G. Bonanno, et al., IEEE Sensors Journal 14 (2014) 3567. http://dx.doi.org/10.1109/JSEN.2014.2328623.